



Finite Element Analysis of Reinforced Self Consolidation Concrete Beams Having a Horizontal Construction Joint

Muhaj Mustafa Abdulmunaam¹, Omar Shamal Farhan²

Authors affiliations:

1) Asst. Chief Eng., Ministry of Construction, Housing and Public Municipalities, Baghdad, Iraq
Eng.muhajmustafa@gmail.com

2*) Asst. Prof. of Structural Eng., Dept. of Architecture Engineering, Al-Nahrain University, Baghdad, Iraq
dr.omer.shamal@nahrainuniv.edu.iq

Paper History:

Received: 26th Aug. 2021

Revised: 2nd Mar. 2022

Accepted: 8th Jul. 2024

Abstract

Construction joints are separations between successive concrete pours. They are critical in the building of large concrete structures, since these structures cannot be cast in a single pour. Self-consolidation concrete is a relatively new kind of concrete that is considered suitable for a wide range of construction applications, especially those needing a high early resistance. Certain findings from earlier experimental tests were adopted and analyzed using finite element analysis. ANSYS program was used to analyze the impact of utilizing high strength concrete (f_c') and the secondary reinforcement ratio (ρ_v) on the behavior of reinforced self-consolidating concrete beams having a horizontal construction joint. Nine beams analyzed in this study have the same dimensions (150×180×1200) mm (width× height ×length). Between the two supports, the clear span was 1100 mm. Two-point loads were applied to the simply supported beams during testing. One of the beams acts as a control beam (without a construction joint) and the remaining beams were with horizontal construction joint in the tension zone. The ultimate loads obtained analytically vary by between 3.1% and 7.8 % from those found experimentally. The presence of the horizontal construction joints made the beam less stiff. Utilizing a 70 MPa high strength concrete resulted in a 47.4 % in ultimate load over the experimental value for regular strength concrete (28 MPa). Increasing the ratio of secondary reinforcement (0.01229 to 0.049) resulted in a 10.3% increase in ultimate load magnitude, while decreasing the ratio of secondary reinforcement (0.01229 to 0.0025) with spanning the spacing between stirrups led to a reduction in ultimate load magnitude by 55.8%.

Keywords: Construction Joints, Self-Consolidating Concrete, ANSYS, Finite Element.

تحليل العتبات الخرسانية المسلحة ذاتية الرص الحاوية على مفاصل انشائية افقية باستخدام طريقة العناصر المحددة
محم مصطفى عبدالمعتم ، عمر شمال فرحان

الخلاصة:

الفواصل الانشائية : هي فواصل بين صب الخرسانة المتتالية وتعتبر ضرورية في بناء الهياكل الخرسانية الكبيرة ، حيث لا يمكن صب هذه الهياكل في مرة واحدة. ان الخرسانة ذاتية الرص هي نوع جديد نسبياً من الخرسانة التي تعتبر مناسبة لمجموعة واسعة من تطبيقات البناء ، خاصة تلك التي تحتاج إلى مقاومة عالية في وقت مبكر . تم اعتماد وتحليل نتائج معينة من الاختبارات التجريبية السابقة باستعمال تحليل العناصر المحددة (finite element analysis) حيث تم استعمال برنامج ANSYS لتحليل تأثير استخدام خرسانة ذات مقاومة انضغاط عالية (f_c') ونسب متغيرة من كمية حديد التسليح الثانوي (ρ_v) على سلوك العتبات الخرسانية المسلحة ذاتية الرص التي لها فواصل إنشائية أفقية. تسع عتبات تم تحليلها في هذه الدراسة لها نفس الأبعاد (150×180×1200) مم (عرض× ارتفاع ×طول). بين الدعامتين ، التمسار الواضح كان 1100 مم. تم تطبيق حملين نقطيين على الكمرات المدعومة ببساطة أثناء الاختبار. واحدة من الكمرات تعمل ككمر تحكم (بدون وصلة إنشائية) والكمرات المتبقية كانت ذات وصلة إنشائية أفقية في منطقة الشد. الأحمال النهائية التي تم الحصول عليها تحليلياً تختلف بين 3.1% و 7.8% عن تلك التي تم العثور عليها تجريبياً. وجود الوصلات الإنشائية أفقية جعلت الكمر أقل صلابة. استخدام خرسانة عالية القوة (70 ميجا باسكال) أسفرت عن زيادة 47.4% في الحمل النهائي مقارنة بالقيمة التجريبية لخرسانة القوة العادية (28 ميجا باسكال). زيادة نسبة التسليح الثانوي (0.01229 إلى 0.049) أسفرت عن زيادة 10.3% في مقدار الحمل النهائي ، في حين أن تقليل نسبة التسليح الثانوي (0.01229 إلى 0.0025) مع تغطية المسافة بين التماسكات أسفرت عن انخفاض مقدار الحمل النهائي بنسبة 55.8%.



× ١٨٠ × ١٢٠٠) مم (العرض × الارتفاع × الطول) وكان طول الفضاء الصافي بين المساند ١١٠٠ ملم وتم تسليط الأحمال على النماذج بتحديد نقطتين على هذه العتبات أثناء الاختبار. ان العتبة الاولى كانت بدون مفصل بناء و العتبات المتبقية كانت مع مفصل بناء أفقي في منطقة الشد. حيث تختلف الأحمال النهائية التي تم الحصول عليها تحليليًا بنسبة تتراوح بين ٣,١٪ و ٧,٨٪ عن تلك التي تم العثور عليها تجريبيًا. وان وجود فواصل انشائية افقية في العتبة ادى الى تصرفها بمتانة اقل. أدى استعمال خرسانة ذات قوة انضغاط عالية (٧٠) ميجا باسكال إلى زيادة في الحمل الاقصى بمقدار ٤٧,٤٪ نسبة لقيمة الحمل الاقصى للخرسانة العادية (٢٨ ميجا باسكال) المستخدمه في التجربة. وايضا عند زيادة نسب التسليح الثانوي من (٠,١٢٢٩ الى ٠,٠٤٩) تم الحصول على زيادة قدرها ١٠,٣٪ في مقدار الحمل الاقصى ، بينما أدى تقليل نسبة التسليح الثانوي من (٠,١٢٢٩ الى ٠,٠٢٥) مع زيادة المسافة بين التسليح الشاقولي (stirrups) إلى تقليل مقدار الحمل الاقصى بنسبة ٥٥,٨٪.

الكلمات المفتاحية: المفاصل الانشائية، الخرسانة ذاتية الرص، ANSYS, طريقة العناصر المحددة

1. Introduction

Due to changes in temperature and moisture content, concrete may shrink or expand, resulting in movement. This implies that the majority of concrete structures need a variety of joints in order to maintain the building's normal operations and to conform to the building's overall design. In general, joints are classified into two types: [1]

- Functional joints allow movement between concrete segments and are utilized for temperature change, shrinkage during setting, expansion, warping, and other purposes.
- Construction joints (CJ): These joints are used to separate concrete segments rather than to enable movement. CJ are breaking points in the concrete placement process since it is impractical to replace concrete in one continuous operation in many frameworks. The primary issue in joint placement is the availability of sufficient shear transition and flexural continuity across the joint. Continuous reinforcement is utilized at the joint to ensure flexural continuity, while dowel reinforcement or shearing friction between new and old concrete contact is used to assist in transferring shearing forces.

Self-consolidation concrete (SCC) a concrete that, in its fresh state, may exhibit amazing deformation and uniformity. A compact, homogeneous, void-free mass is formed by its own weight without external vibration [2]. Due to the great flowability and operational value of this kind of concrete, it enables the production of concrete molds with dense reinforcement proportions without concern of segregation since it solidified under its own weight without the need for vibration.

The finite element method (FEM) is a numerical analytical technique for approximating solutions to a wide variety of engineering problems. ANSYS software offers engineers a variety of enhanced features and tools that enable them to do their jobs more effectively. It is used in structures, aerospace, electronics, and nuclear energy.

Yousifani in 2004 [3], investigated the behavior of reinforced concrete beams with CJ using nonlinear

three-dimensional finite elements. A parametric study was presented, including the kind of joint (vertical or horizontal), the joint's position, the interface's coefficient of friction, and the proportion of steel in the joint. Two beams were suggested for investigation of the aforementioned conditions. They were evaluated by using vertical or horizontal structural joints in various places. A study of the beams' behavior and load-carrying capability indicated that vertical joint effects were small (the percentage of reduction in ultimate load capacity is in the range of 0 % - 10%). While the horizontal construction joints have a significant impact on the overall performance and load-carrying capacity of the structure (the percentage of reduction in ultimate load capacity is in the range of 6 %- 20%).

Abdul-Majeed in 2010 [4], presented a study on the evaluation of transverse CJ of reinforced concrete beams. The present research evaluated available experimental data using the nonlinear three-dimensional finite element ANSYS computer software (v. 9). Additionally, an interface model for the transverse CJ was suggested. Six beams with varying transverse CJ at mid-span are examined, as well as one reference beam without a joint. The findings indicated that:

- The nonlinear finite element technique of analysis is a strong and reasonably inexpensive tool for estimating the structural reaction and load bearing capability of reinforced concrete members.
- The shape of the transverse construction joint influenced the strength, ductility, and failure mode of jointed reinforced concrete beams.
- Using interface elements to link concrete brick elements simulates joint weakness and assesses stress transmission via the joint.
- Adding one stirrup across the vertical joint increase performance, strengthens the joint, and stops crack propagation.

Abdul-Majeed and et al in 2010 [5], studied the effect of the number of horizontal construction joints (HCJ) on reinforced concrete beams. The analysis



included three beams with one, two, and three (HCJ) joints that split the beam into equal parts, as well as one reference beam without a joint. The results of the finite element analysis were in excellent agreement with those of the prior experimental tests. For all kinds of tested beams, the greatest variation in ultimate loads was about (8.2-10.4) %. The existence of one, two, and three (HCJ) in RC beams subjected to flexure resulted in a reduction in the value of the cracking load, such that P_{cr} was (97 %, 85%, and 80% respectively) compared to the reference beam. When compared to the reference beam, the ultimate load capacity of Pult was (96%, 89%, and 84% respectively).

Based on the aforementioned reviews, we found a gap in the studies that deal with finite element analysis of SCC beams with construction joints.

2. Verification of Experimental Data

This study was analyzed according to previous experimental test results to investigate the effect of using high strength concrete (f_c') and the effect of the secondary reinforcement ratio (ρ_v) on the behavior of reinforced SCC beams. The dimensions of all the beams analyzed in the experimental study were the same (150 mm width, 180 mm height, and 1200 mm length). The clear span between the two supports was 1100 mm. The simply supported beams were subjected to two point loads. These specifications were also used by the analysis using the ANSYS program to model the nine beams. One of the beams acts as a control beam (without a construction joint) and the remaining beams have a horizontal construction joint in the tension zone at 55 mm from the bottom of the beam. Figures (1) illustrate the beam geometry, whereas figures (2) show the CB and B1 FEM.

3. ANSYS Material Modeling

3.1 Concrete Modeling

The concrete was modeled using Solid 65 (eight-node solid element). Each node in the solid element has three degrees of freedom: translations in the x, y, and z dimensions. This element's properties include cracking in tension, crushing in compression, creep nonlinearities, and high deflection geometric nonlinearities. Also, the element may be used to test unreinforced concrete members [6]. In Figure (3), the element shape and the node locations are shown.

Figure (4) depicts a typical uniaxial stress-strain curve generated by ANSYS. You can observe that the concrete acts linearly up to $(0.3 f_c')$, then gradually increases in curvature up to $(0.75 f_c')$, then falls after reaching f_c' until the concrete crushes at ultimate strain.

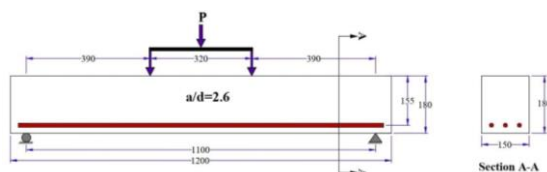
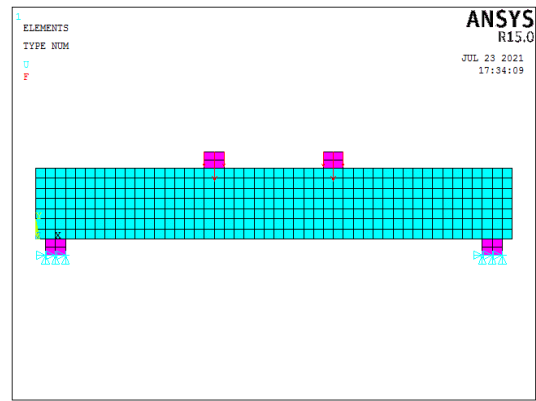
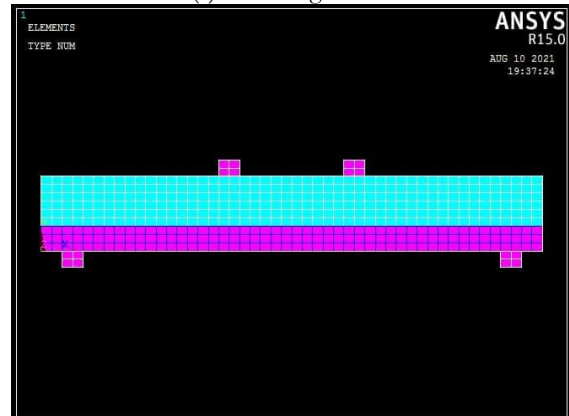


Figure (1): Beam Geometry used in the Study.



(a) Modeling of CB



(b) Modeling of B1

Figure (2): Finite element mesh used (a) modeling of CB (b) modeling of b1

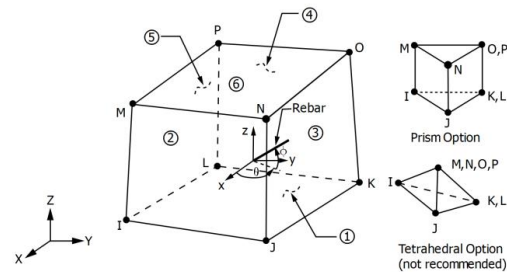


Figure (3): SOLID 65 element geometry [6].

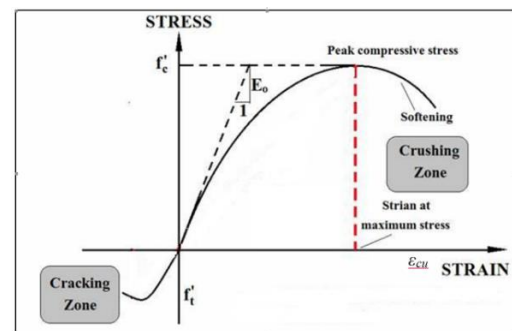


Figure (4): Typical uniaxial compressive and tensile stress-strain for concrete [8].

The tension-stiffening effect is being investigated because cracked concrete may initially sustain certain tensile stresses in the direction normal to the crack. This was achieved in ANSYS-16 by assuming a gradual release of the concrete stress component normal to the cracked plane. The normal stress that cracked concrete



can withstand may be estimated in this research by referring to Figure (5). [7]

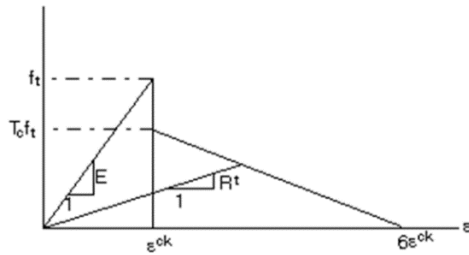


Figure (5): Concrete post cracking model [7].

A smeared crack approach is used for crack modeling in computer program (ANSYS-16). This method eliminates the need for new meshes for cracks that form and spread, which lowers computing complexity as shown in Figure (6)

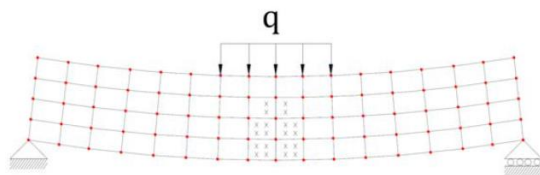


Figure (6): Smeared crack model [9].

3.2 Steel Reinforcement Modeling

Link-8 is a spar that may be used in a variety of engineering applications. A spar element may mimic trusses, drooping cables, linkages, and springs. The three-dimensional spar element allows translations in the nodal x, y, and z dimensions. The element is defined by two nodes, the cross-sectional area, an initial strain, and the material properties. The element's x-axis spans along its length, from node I to node J. This element was used to represent steel reinforcement [6]. The geometry of this element is shown in Figure (7).

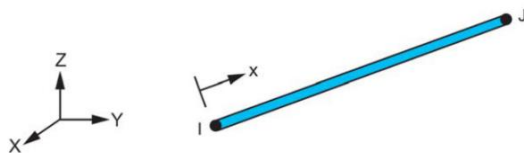


Figure (7): LINK-8 spar element [6].

A discrete representation was used to simulate the longitudinal and transverse reinforcements. Because the individual elements are generated during modeling through nodes, there is no need for a mesh for the reinforcement. The discrete steel method and the reinforcement model for CB are shown in figures (8) and (9) below.



Figure (8): Discrete method to represent reinforcement [10].

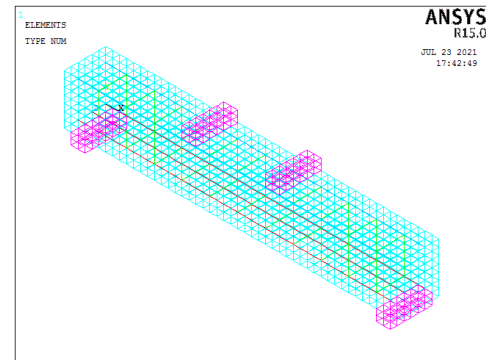


Figure (9): Steel reinforcement representation at CB.

In the ANSYS computer program, the behavior of steel bar is represented as a bilinear stress-strain curve starting in the region with positive stress and strain values. The uniaxial stress-strain relationship of the steel is represented as a bilinear curve, suggesting that it is elastic-plastic with strain hardening. As a consequence, it disregards upper yield points and strain hardening. In the ANSYS program, the figure (10) depicts a typical uniaxial stress-strain curve for a steel reinforcement.

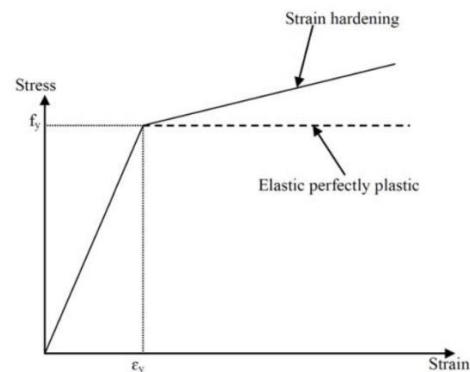


Figure (10): Typical stress-strain diagram. [11].

3.3 loading and support steel plates modeling

Steel plates were inserted at support and loading locations in the finite element models to avoid stress concentration and local failure. In three dimensions, the solid 45 is used to depict structural elements. Eight nodes constitute the element, each of which has three degrees of freedom, enabling translations in the nodal x, y, and z directions. The element's properties include plasticity, creep swelling, stress stiffening, large deflection, and large strain [6]. The form, node locations, and coordinate system of this element are shown in Figure (11). The dimension of these plates used in this study were (50 mm width, 150 mm length, and 40 mm thick). Figure (12) displays the boundary and loading conditions in CB.

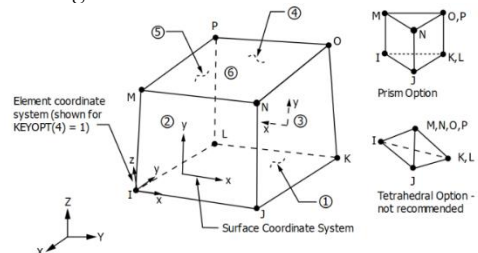


Figure (11): Solid 45 element geometry [6].

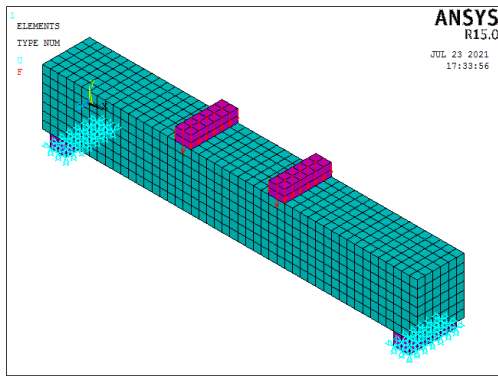


Figure (12): CB loading and boundary conditions plates.

3.4 Horizontal Construction Joint Modeling (interface modeling)

An interface connects two distinct concretes. In these conditions, the concept of concrete-to-concrete interface load transfer is critical in assuming the monolithic behavior of the resulting composite reinforced concrete components. We must investigate the transmission of three types of forces: tension force, compression force, and shear force [12]. According to Randal [13], whereas external tensile forces are transferred through reinforcement across the interface, compression forces directly pass through the concrete. The main goal is to ensure that shear forces are transferred along the joint. Mechanical interlock, adhesive bonding, friction, or dowel action may all be used to describe the mechanism of interface shear transfer.

In this study, the interaction at interfaces was modeled using two combinations of interface models. The first interface is capable of withstanding just compression forces normal to the contact surface and tangential shear (Coulomb friction). TAUMAX is the highest contact friction stress that may be given without causing sliding regardless of the amount of normal contact pressure applied. $TAUMAX = \sqrt{fc'}$ MPa is chosen in this research as a consequence of the findings in reference [7]. This interface model was idealized using the CONTA172 and TARGE169 two-dimensional surface-to-surface contact elements.

3.4.1 CONTA172

CONTA172 specifies the contact and sliding between two-dimensional target surfaces (TARGE169) and a deformable surface. The element may be utilized in studies of two-dimensional structural and coupled-field contacts. It is appropriate for pair-based as well as general interaction. In the case of pair-based contact, the target surface is defined by the 2-D target element type, TARGE169. In the case of general contact, the target surface may be defined using either CONTA172 elements (for deformable surfaces) or TARGE169 elements (for rigid bodies only). When an element surface penetrates an associated target surface and has the same geometric characteristics as the solid element face with which it is connected, contact occurs. Coulomb friction, shear stress friction, user-defined friction with the USERFRIC subroutine, and user-defined contact interaction with the USERINTER function are all available. This element

also allows for bonded contact separation, which simulates interface delamination [6]. Figure (13) shows the geometry of this element and figure (14) displays the interface layer used in B1 (beam with HCJ at tension zone).

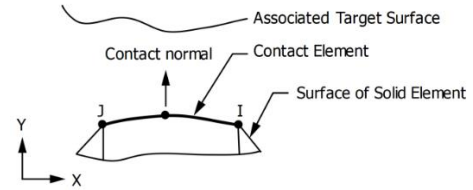


Figure (13): CONTA172 element [6].

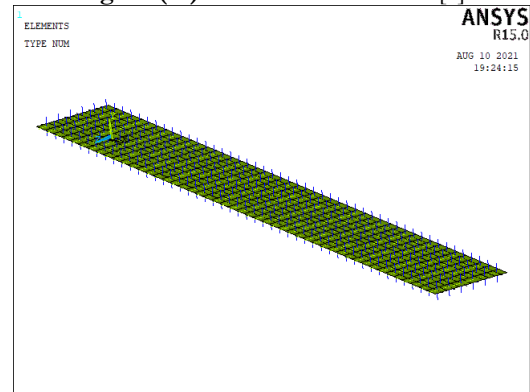


Figure (14): B1 interface (HCJ) modeling in ANSYS.

3.4.2 TARGE169

TARGE169 is used to represent various two-dimensional "target" surfaces for the contact components that are linked to it (CONTA171, CONTA172, and CONTA175). The contact elements are placed on the solid components that define the boundary of a deformable body and may come into touch with the TARGE169, target surface. We may apply any translational or rotational displacement, voltage, magnetic potential, temperature, pressures, and moments to the target segment element [6]. Figures (15) depict the geometry of TARGE169.

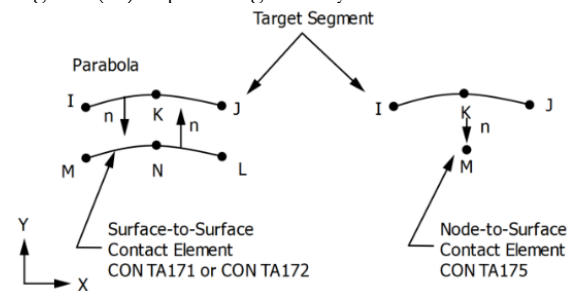


Figure (15): Geometry of TARGE169 element [6].

4. Numerical Integration and Nonlinear Solution Procedures

The Gauss quadrature technique is utilized in this study to calculate the integrals required to setup the element stiffness matrix. The integration rule used in this work is the 8 (2×2×2) points rule, Figure (16). The locations of the sampling points and the weighting factors for the 2×2×2 integration rule are shown in Table (1).

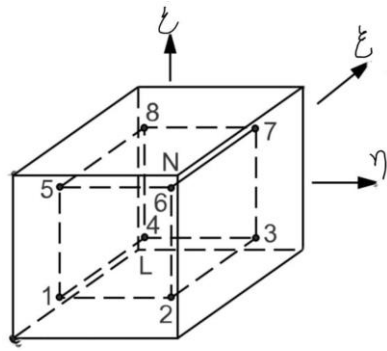


Figure (16): Brick element/integration points location [6].

Table (1): Sampling Points Position and Weighting Factor for $2 \times 2 \times 2$ Gauss Quadrature [6] [14]

Sampling Point	Position of points			Weight
	ξ	η	ζ	
1-8	± 0.57734	± 0.57734	± 0.57734	1

The ANSYS software used incremental-iterative solution methods with the Newton-Raphson algorithm. As illustrated in Figure (17), the load is applied gradually, and iterations are performed to obtain a converged solution matching to the loading stage under consideration.

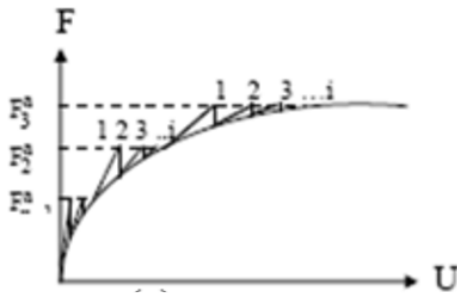


Figure (17): Incremental-iterative method [7].

5. Finite Element Results

5.1 Load and Deflection at Failure

Figure (18) depicts the finite element analysis (ANSYS) deflection and ultimate load findings for the control beam at failure. The FEA load at failure for the CB and B1 were (163.25 kN, and 150 kN respectively) whereas the failure load determined from experiment was (170 kN, and 156 kN respectively) resulting in a failure load difference of about (3.9%). Figure (19) and (20) depict the experimental and analytical load-deflection curves for control beam and B1 (CJ at tension zone). The presence of HCJ made the beam less stiff as seen in the figure (21).

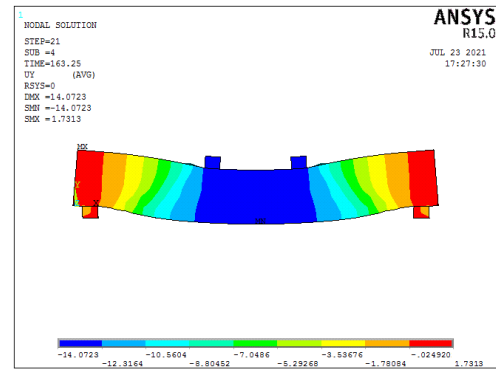


Figure (18): Failure load and deflection for CB.

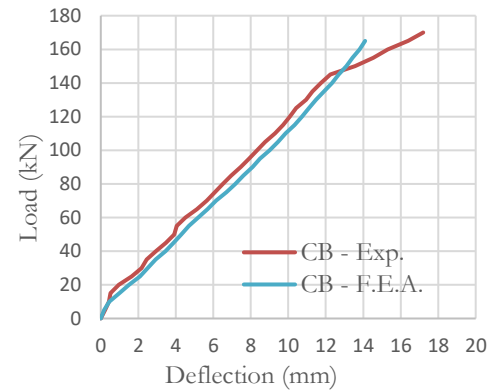


Figure (19): load-deflection curves for CB.

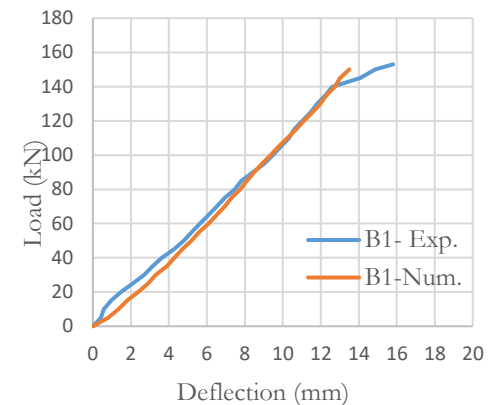


Figure (20): load-deflection curves for B1.

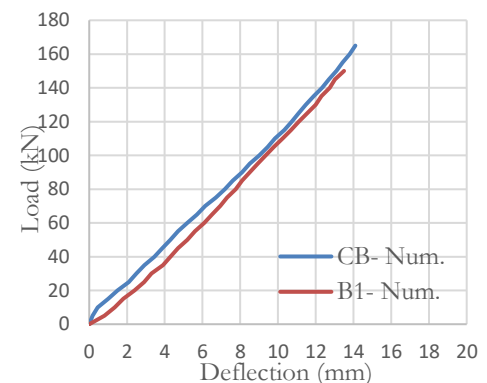


Figure (21): load-deflection curves for CB and B1.

5.2 Crack Patterns

The fractured cracking or crushing types of fracture that occur in concrete components are indicated by circles inserted at sampling points in the ANSYS computer program. The following are the classifications of crack and crush fractures:



1. A circular outline in the fracture plane indicates the presence of cracking.
2. An octahedron represents crushing.
3. If a fracture has been opened and then closed, an X will be drawn over the circular outline's matching circle.

The integration point of each brick element may fracture into up to three different planes. A red circle outline denotes the first crack, a green circle outline denotes the second crack, and a blue circle outline denotes the third crack [6]. The fracture pattern of the control beam at the ultimate analytical load (163 kN) is shown in Figure (22).

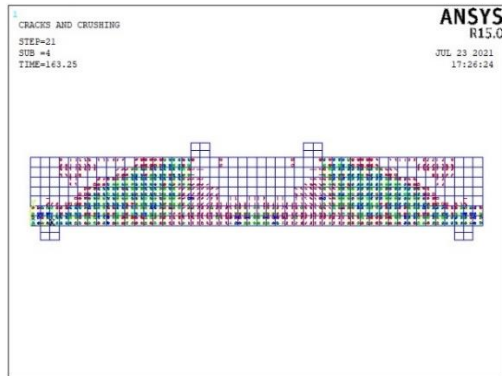


Figure (22): CB Cracks pattern in FEA at ultimate load.

5.3 Stress Distribution for concrete

The distribution of concrete stress for CB at the ultimate load is shown in Figure (23). At mid-span, when the top fibers of the cross section are under compression and the bottom fibers are under tension, the higher compressive stresses are clearly apparent. The compressive stress with the greatest value recorded (-26.57 MPa) is directly under the applied load.

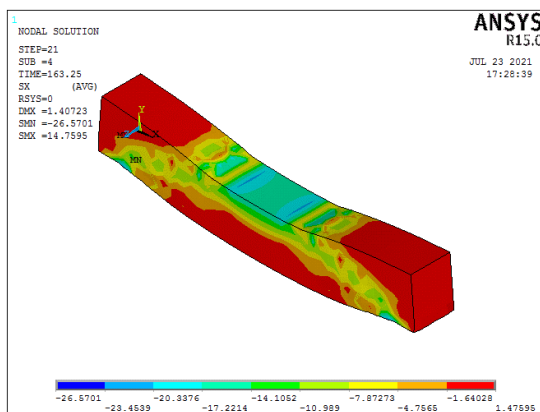


Figure (23): Stress distribution in concrete for cb at ultimate load.

5.4 Stresses in Steel Reinforcement

Strain gauges were installed on the steel reinforcing bars at the locations where the experimental program required stress measurements. However, calculating the stress distribution along steel bars is a time-consuming process that may be replaced by virtual strain (and stress) gauges produced via finite element analysis. Steel stresses in four stirrups (from right) of a control beam between the applied load and the support

area are shown in figures (24) and figure (25) below. The yield stress of the 4 mm stirrups used in CB was (640 MPa), indicating that none of the stirrups have reached their yield point. The maximum stress measured in the middle stirrups (3rd) between load and support was about 440 MPa. Noticing that during the experiment, the stirrups' yield point was exceeded.

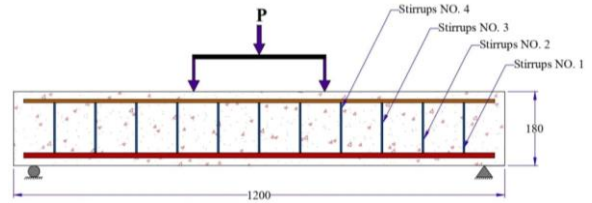


Figure (24): Steel stirrups used in CB to locate stresses.

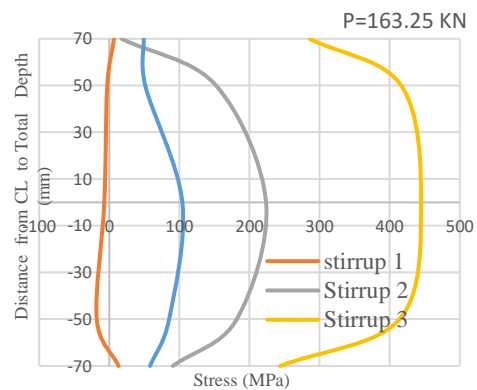


Figure (25): Steel stresses for the first 4th stirrups.

6. Parametric Study for Experimental Data

The beam designated as (B1) that studied in the preceding article was chosen for parametric study to determine the effect of various material and solution variables on the behavior of reinforced SCC beams in the presence of CJ. The impact of concrete compressive strength and stirrup reinforcement were considered.

6.1 Effect of Concrete Compressive Strength (f_c')

In this study, the compressive strength of concrete (f_c') for beam B1 was found to be 21, 28, 47, and 70 MPa. It is clear that as the compressive strength of concrete rises, so does the ultimate load. Table 2 shows the numerical ultimate loads obtained for different concrete grades in the analyzed beam and compared to the experimental B1.

Table (2): Effect of Grade of Concrete at the Ultimate Load of B1

Value of (f_c') MPa	Numerical ultimate load (kN)	Pult Num../ Pult FEM *	Pult Num../ Pult Exp. **
21	83	0.55	0.53
28	150	1	0.96
47	157	1.05	1.01
70	230	1.53	1.47

* Pult FEM = 230 kN (f_c' =28 MPa)

**Pult_{exp} = 156 kN (f_c' = 28 MPa)



6.2 Effect of Stirrup Reinforcement.

In this research, the secondary reinforcement (stirrups) ratio for B1 was found to be 0.0025, 0.0031, 0.01229, 0.0276, and 0.049 at compressive strength 28 MPa. The ultimate load clearly increases as the secondary reinforcement ratio of concrete increases. Table (3) illustrates the numerical ultimate loads computed for various secondary reinforcement ratios for concrete in the analyzed beam to the experimental B1.

Table (3): Effect of Secondary Reinforcement Ratio at Ultimate Load of B1

Value of ρ_v	Numerical ultimate load (kN)	Pult Num./Pult FEM *	Pult Num./Pult Exp. **	
B1	0.0025	69	0.46	0.44
	0.0031	74	0.49	0.47
	0.01229	150	1	0.96
	0.0276	155	1.03	0.99
	0.049	172	1.15	1.1

* Pult FEM = 230 kN ($f_c' = 28$ MPa)

** Pult exp = 156 kN ($f_c' = 28$ MPa)

7. Conclusion

- The analytical program's ultimate loads were lower than the experimental program's findings. The difference was 3.1 % -7.8 %.
- The presence of the HCJ made the beam more ductile.
- The crack patterns generated by numerical analysis at the failure loading stage agree well with the experimental failure results.
- Stresses in steel secondary reinforcement for CB did not reach its yield point. The maximum stress reached was about 440 MPa while the yield stress of the actual stirrups equal 640 MPa, noticing that in the experimental results the stirrups exceeds its yield point.
- According to the parametric study of experimental data, employing a high strength concrete of 70 MPa resulted in a 47.4 % in ultimate load above the experimental value with normal strength (28 MPa).
- In a parametric study of experimental data, using 8 @100 mm with $\nu = 0.049$ led to a 10.3 % in ultimate load value, whereas using 2mm @125 mm with $\nu = 0.0025$ resulted in a 55.8 % reduction in ultimate load magnitude.

8. References

- [1] M. Fintel, *Handbook of Concrete Engineering*, New York, NY, USA: Van Nostrand Reinhold Company, 1985.
- [2] H. Okamura and M. Ouchi, "Self-Compacting Concrete," *J. Adv. Concr. Technol.*, vol. 1, no. 1, pp. 5-15, Apr. 2003.
- [3] A. H. Yousifani, "Investigation of the Behavior of Reinforced Concrete Beams with Construction Joints Using Nonlinear Three-Dimensional Finite Elements," Master's thesis, College of Engineering, University of Technology, Baghdad, Iraq, 2004.
- [4] Q. Abdul-Majeed, "Evaluation of Transverse Construction Joints of Reinforced Concrete Beams," *Eng. Technol. J.*, vol. 28, no. 14, pp. 4750-4773, 2010.
- [5] Q. Abdul-Majeed, L. A. Ghaleb, and M. G. Ghaddar, "Effect of the Number of Horizontal Construction Joints in Reinforced Concrete Beams," *Engineering and Technology Journal*, vol. 28, no. 19, 2010.
- [6] ANSYS, "ANSYS Help," Release 15.0, n.d.
- [7] O. S. Farhan, "Behavior of Self Compacting Concrete Deep Beams under Repeated Loading," Ph.D. thesis, College of Engineering, AL-Nahrain University, 2014.
- [8] M. Y. H. Bangash, *Concrete and Concrete Structures: Numerical Modeling and Applications*, Essex, England: Elsevier Science Publishers, 1989.
- [9] R. N. Hamedani and M. S. Esfahani, "Numerical Evaluation of Structural Behavior of the Simply Supported FRP-RC Beams," Master's thesis, Royal Institute of Technology (KTH), Stockholm, Sweden, 2012.
- [10] K. T. Chong, "Numerical Modeling of Time-Dependent Cracking and Deformation of Reinforced Concrete Structures," Doctoral thesis, University of New South Wales, Sydney, Australia, 2004.
- [11] T. Supaviriyakit, P. Pornpongsaroj, and A. Pimanmas, "Finite element analysis of FRP-strengthened RC beams," *Songklanakarinn J. Sci. Technol.*, pp. 498-507, 2004.
- [12] F. Z. Gigar, "Experimental Investigation of Construction Joints in RC Beams," M.S. thesis, Addis Ababa Univ., Addis Ababa, Ethiopia, 2015.
- [13] N. Randl, "Design recommendations for interface shear transfer in MC 2010," Ernst & Sohn, pp. 230-241, 2013. doi: 10.1002/suco.201300003.
- [14] D. J. Dawe, *Matrix and Finite Element Displacement Analysis of Structures*, Clarendon Press, Oxford, U.K., 1984.